Transition-Metal Complexes with Sulfur Ligands. 82.[1] H_2S, S_2, and CS_2 Molecules as Ligands in Sulfur-Rich [Ru(PPh$_3$)('S$_4$')] Complexes ('S$_4$'$^{2-}$ = 1,2-Bis[(2-mercaptophenyl)thio]ethane(2-))

Dieter Sellmann,* Peter Lechner, Falk Knoch, and Matthias Moll

Contribution from the Institut für Anorganische Chemie der Universität Erlangen-Nürnberg, Egerlandstrasse 1, D-8520 Erlangen, Federal Republic of Germany. *Received June 5, 1991*

Abstract: Red [Ru(PPh$_3$)'S$_4$']$_x$ ('S$_4$'$^{2-}$ = 1,2-bis[(2-mercaptophenyl)thio]ethane(2-)) reacts in liquid H_2S at -70 °C to give [Ru(SH$_2$)(PPh$_3$)'S$_4$'] (**1**) which recrystallizes from H_2S-saturated THF as **1**·THF in yellow-orange single crystals. Crystals of **1**·THF are monoclinic, space group $P2_1/c$, with a = 1124.7 (9) pm, b = 1378.5 (14) pm, c = 2274.0 (16) pm, β = 97.06 (6)°, V = 3499 (5) × 10^6 pm^3, Z = 4, and R_w (R) = 0.056 (0.065) for 3366 reflections. **1**·THF is the first of the rare and often very unstable H_2S complexes that could be characterized by X-ray crystallography and shows how H_2S in complexes with sulfur-dominated coordination spheres is stabilized by hydrogen bonds. **1** and **1**·THF are rapidly oxidized by O_2 to yield deep turquoise-blue [(μ-S$_2$){Ru(PPh$_3$)'S$_4$'}$_2$] (**2**) which has a trans η^1-η^1-S_2 bridge and exists in two diastereomeric forms as proved by X-ray structure determination of **2**·CH_2Cl_2 and **2**·CS_2. Crystals of **2**·CH_2Cl_2 are triclinic, space group $P\bar{1}$, with a = 999.5 (5) pm, b = 1043.7 (7) pm, c = 1672.4 (14) pm, α = 78.89 (6)°, β = 89.46 (5)°, γ = 75.43 (5)°, V = 1655 (2) × 10^6 pm^3, and Z = 1. Due to unsatisfactory crystal quality, the structure could not be fully refined. Crystals of **2**·CS_2 are monoclinic, space group $P2_1/c$, with a = 2695.6 (10) pm, b = 1289.9 (4) pm, c = 1947.7 (6) pm, β = 105.66 (3)°, V = 6519 (4) × 10^6 pm^3, Z = 4, and R_w (R) = 0.068 (0.079) for 7754 reflections. The RuSSRu core in **2** is a chromophore and is described as delocalized 4c-6e π system. A high degree of sulfur coordination at the Ru centers is assumed to be responsible for the unusual electronic properties of **2** compared with other μ-S_2 complexes. Addition of CS_2 to [Ru(PPh$_3$)'S$_4$'] fragments leads to formation of binuclear deep red [{Ru(PPh$_3$)}(μ-'S$_4$'CS$_2$){Ru(PPh$_3$)'S$_4$'}] (**3**; 'S$_4$'CS$_2$$^{2-}$ = 2-[[2-[(2-mercaptophenyl)-thio]ethyl]thio]phenyl trithiocarbonate(2-)) that exists in two diastereomeric pairs of enantiomers. One pair was characterized by X-ray crystallography of **3**·CS_2 that contains a bridging thioxanthate ligand in an unprecedented bonding mode. Crystals of **3**·CS_2 are monoclinic, space group $P\bar{1}$, with a = 1352.9 (6), b = 1414.9 (10), c = 1848.4 (17) pm, α = 76.79 (6)°, β = 68.87 (5)°, γ = 85.93 (5)°, V = 3211 (4) × 10^6 pm^3, Z = 2, and R_w (R) = 0.082 (0.104) for 3954 reflections.

Introduction

The interaction of H_2S, HS^-, and S^{2-} with transition metals is widespread in nature and responsible for the formation of ores as well as [M_xS_y] clusters in active centers of redox enzymes like ferredoxines or nitrogenases. Hence, transition-metal complexes with such sulfur ligands are of great interest with regard to model compounds for these metal enzymes.[2]

In contrast to the numerous and often very stable complexes with S^{2-} ligands, complexes with ligands containing SH functions are rare and labile.[3,4a] H_2S complexes[4a-g] could be isolated only in exceptional cases. They were never studied by X-ray crystallography and differ in this respect remarkably from the homologous H_2O complexes. Reasons might be the great reactivity of H_2S and HS^- ligands leading to fast consecutive reactions as well as the high tendency of formation of sulfide-bridged structures.[3,4a]

S_2 units are potential oxidation products of H_2S ligands. S_2 molecules in the free state are unstable, but S_2 ligands have been proved in a number of complexes. Bridging of metal centers by trans η^1-η^1-S_2 units is relatively rare[3] and could be characterized by X-ray crystallography only in [(μ-S$_2$){Ru(NH$_3$)$_5$}$_2$]Cl$_4$·2H$_2$O,[5] [(μ-S$_2$){Mn(Cp)(CO)$_2$}$_2$],[6] [(μ-S$_2$)$_2$[Ru(MeCp)(PPh$_3$)]$_2$],[7] and [(μ-S$_2$){Ru(Cp)(PMe$_3$)$_2$}$_2$](BF$_4$)$_2$,[8] which exhibit metal centers with abiological coordination spheres.

Heterocumulene CS_2 is also highly reactive. Its chemistry in the coordination spheres of transition-metal complexes is currently intensively investigated. Coordination, insertion, addition, and cleavage reactions of CS_2 are of interest, also with respect to reactions of the structurally closely related CO_2.[9]

In this work we report syntheses, structures, and reactions of [Ru(SH$_2$)(PPh$_3$)'S$_4$'] (**1**) and [(μ-S$_2$){Ru(PPh$_3$)'S$_4$'}$_2$] (**2**) ('S$_4$'$^{2-}$ = 1,2-bis[(2-mercaptophenyl)thio]ethane(2-)) and [{Ru-(PPh$_3$)}(μ-'S$_4$'CS$_2$){Ru(PPh$_3$)'S$_4$'}] (**3**) ('S$_4$'CS$_2$$^{2-}$ = 2-[[2-[(2-mercaptophenyl)thio]ethyl]thio]phenyl trithiocarbonate(2-)). Preliminary results were reported elsewhere.[2,10]

* To whom correspondence should be addressed.

Experimental Section

General Procedures. Unless noted otherwise, all reactions and operations were carried out under nitrogen with exclusion of light at room temperature by using standard Schlenk techniques. Solvents were dried and distilled before use. [Ru(PPh$_3$)'S$_4$']$_x$ was prepared as described in the literature.[11] H_2S was purchased in lecture bottles from Gerling, Holz & Co., Hanau, Germany. Spectra were recorded on the following instruments: IR, Zeiss IMR 25 and Perkin-Elmer 983; NMR, JEOL JNM-GX 270 and JNM-EX 270; UV-vis-near-IR, Shimadzu UV-3101 PC; Mass spectra, Varian MAT 212. Magnetic moments of solids were determined on a Johnson Matthey magnetic susceptibility balance at room temperature.

(1) Part 81: Sellmann, D.; Geck, M.; Moll, M. Z. *Naturforsch.*, in press.
(2) Sellmann, D.; Barth, I. *Inorg. Chim. Acta* **1989**, *164*, 171 and literature reported therein.
(3) (a) Müller, A.; Jagermann, W. *Inorg. Chem.* **1979**, *18*, 2631. (b) Müller, A.; Diemann, E. In *Comprehensive Coordination Chemistry*; Wilkinson, G., Gillard, R. D., McCleverty, J. A., Eds.; Pergamon Press: Oxford, 1987; Vol. 2, p 531.
(4) (a) [Ru(NH$_3$)$_5$(SH$_2$)](BF$_4$)$_2$ and [Ru(isn)(NH$_3$)$_4$(SH$_2$)](BF$_4$)$_2$ (isn = isonicotinamide): Kuehn, C. G.; Taube, H. *J. Am. Chem. Soc.* **1976**, *98*, 689. (b) [M(CO)$_5$(SH$_2$)] (M = W, Cr): Herberhold, M.; Süss, G. *Angew. Chem.* **1976**, *88*, 375; *Angew. Chem., Int. Ed. Engl.* **1976**, *15*, 366. (c) [Mn(CO)$_4$(PPh$_3$)(SH$_2$)]BF$_4$: Harris, P. J.; Knox, S. A. R.; McKinney, R. J.; Stone, F. G. A. *J. Chem. Soc., Dalton Trans.* **1978**, 1009. (d) [CpMo(CO)$_3$(SH$_2$)]BF$_4$ and [CpW(CO)$_3$(SH$_2$)]AsF$_6$: Urban, G.; Sünkel, K.; Beck, W. *J. Organomet. Chem.* **1985**, *290*, 329. (e) [Re(CO)$_5$(SH$_2$)]BF$_4$: Raab, K.; Beck, W. *Chem. Ber.* **1985**, *118*, 3830. (f) [Pt(PPh$_3$)$_2$(SH$_2$)]: Morelli, D.; Segre, A.; Ugo, R.; La Monica, G.; Genini, S.; Conti, F.; Bonati, E. *J. Chem. Soc., Chem. Commun.* **1967**, 524. (g) [CpRu(PPh$_3$)$_2$(SH$_2$)](OSO$_2$CF$_3$): Amarasekera, J.; Rauchfuss, T. B. *Inorg. Chem.* **1989**, *28*, 3875.
(5) (a) Brulet, C. R.; Isied, S. S.; Taube, H. *J. Am. Chem. Soc.* **1973**, *95*, 4758. (b) Elder, R. C.; Trkula, M. *Inorg. Chem.* **1977**, *16*, 1048. (c) Kim, S.; Otterbein, E. S.; Rava, R. P.; Isied, S. S.; San Filippo, J., Jr.; Waszcyak, J. V. *J. Am. Chem. Soc.* **1983**, *105*, 336.
(6) Herberhold, M.; Reiner, D.; Zimmer-Gasser, B.; Schubert, U. *Z. Naturforsch.* **1980**, *35b*, 1281.
(7) Amarasekera, J.; Rauchfuss, T. B. *Inorg. Chem.* **1987**, *26*, 2017.
(8) Amarasekera, J.; Rauchfuss, T. B.; Wilson, S. R. *Inorg. Chem.* **1987**, *26*, 3328.
(9) Crocq, V.; Daran, J.-C.; Jeannin, Y.; Eber, B.; Huttner, G. *Organometallics* **1991**, *10*, 448.
(10) Sellmann, D.; Lechner, P.; Knoch, F.; Moll, M. *Angew. Chem.* **1991**, *103*, 599; *Angew. Chem., Int. Ed. Engl.* **1991**, *30*, 552.
(11) Sellmann, D.; Barth, I.; Moll, M. *Inorg. Chem.* **1990**, *29*, 176.

0002-7863/92/1514-922$03.00/0

Table I. Selected Crystallographic Data for $[Ru(SH_2)(PPh_3)('S_4')]\cdot THF$ (**1**·THF), $[(\mu\text{-}S_2)\{Ru(PPh_3)('S_4')_2\}]\cdot CH_2Cl_2$ (**2**·CH_2Cl_2), $[(\mu\text{-}S_2)\{Ru(PPh_3)('S_4')_2\}]\cdot CS_2$ (**2**·CS_2), and, $[\{Ru(PPh_3)\}(\mu\text{-}'S_4'CS_2)\{Ru(PPh_3)('S_4')\}]\cdot CS_2$ (**3**·CS_2)

compd	$[Ru(SH_2)(PPh_3)('S_4')]\cdot$ THF (**1**·THF)	$[(\mu\text{-}S_2)\{Ru(PPh_3)('S_4')_2\}]\cdot$ CH_2Cl_2 (**2**·CH_2Cl_2)	$[(\mu\text{-}S_2)\{Ru(PPh_3)('S_4')_2\}\cdot$ CS_2 (**2**·CS_2)	$[\{Ru(PPh_3)\}(\mu\text{-}'S_4'CS_2)\{Ru(PPh_3)('S_4')\}]\cdot$ CS_2 (**3**·CS_2)
formula	$C_{36}H_{37}OPRuS_5$	$C_{65}Cl_2H_{56}P_2Ru_2S_{10}$	$C_{65}H_{54}P_2Ru_2S_{12}$	$C_{66}H_{54}P_2Ru_2S_{12}$
mol wt	778.08	1491.68	1484.03	1496.04
cryst dimens, mm	0.40 × 0.20 × 0.20	0.15 × 0.15 × 0.05	0.30 × 0.20 × 0.10	0.30 × 0.20 × 0.05
space gp	$P2_1/c$	$P\bar{1}$	$P2_1/c$	$P\bar{1}$
cell dimens				
a, pm	1124.7 (9)	999.5 (5)	2695.6 (10)	1352.9 (6)
b, pm	1378.5 (14)	1043.7 (7)	1289.9 (4)	1414.9 (10)
c, pm	2274.0 (16)	1672.4 (14)	1947.7 (6)	1848.4 (17)
α, deg	90.00 (0)	78.89 (6)	90.00 (0)	76.79 (6)
β, deg	97.06 (6)	89.46 (5)	105.66 (3)	68.87 (5)
γ, deg	90.00 (0)	75.43 (5)	90.00 (0)	85.93 (5)
V, pm^3	3499 (5) × 10^6	1655 (2) × 10^6	6519 (4) × 10^6	3211 (4) × 10^6
Z	4	1	4	2
d_{cal}, g/cm^3	1.48	1.49	1.51	1.55
wavelength, pm	71.073	71.073	71.073	71.073
measd temp, K	200	200	200	200
measd reflns	7662	6939	13449	9241
unique reflns	6662	6727	12457	9033
obsd reflns	4759	2227	7754	3954
σ criterion	$F > 6\sigma(F)$	$F > 6\sigma(F)$	$F > 6\sigma(F)$	$F > 6\sigma(F)$
no. parameters	401	204	716	725
R/R_w	0.065/0.056	0.151/0.151	0.079/0.068	0.104/0.082

Preparation of Compounds. $[Ru(SH_2)(PPh_3)('S_4')]\cdot THF$ (1·THF) from $[Ru(PPh_3)('S_4')]_x$. All procedures were carried out in a H_2S atmosphere with strict exclusion of O_2 and H_2O by using H_2S-saturated solvents!

A 10-mL portion of H_2S was condensed onto $[Ru(PPh_3)('S_4')]_x$ (830 mg, 1.24 mmol) at −196 °C in a Schlenk tube. Slow warming of the mixture to −70 °C gave a red suspension, which rapidly turned into a clear yellow solution. Concentration of volume to 1 mL at −60 °C caused precipitation of yellow **1**. Careful dissolution in 30 mL of cold (−50 °C) THF and slow addition of 30 mL of pentane (−10 °C) under rapid stirring yielded microcrystalline **1**·THF which was separated, washed with pentane/THF (10:1), and dried in a stream of H_2S gas for 10 h. Yield: 745 mg (77%). Anal. Calcd for $C_{36}H_{37}OPRuS_5$ (778.08): C, 55.57; H, 4.79; S, 20.61. Found: C, 55.88; H, 4.79; S, 20.45.

$[(\mu\text{-}S_2)\{Ru(PPh_3)('S_4')_2\}]\cdot CH_2Cl_2$ (2·CH_2Cl_2) from 1. A 10-mL portion of H_2S was condensed onto $[Ru(PPh_3)('S_4')]_x$ (955 mg, 1.42 mmol) at −196 °C in a Schlenk tube. The mixture was slowly warmed to −70 °C and stirred until the red suspension had turned into a yellow solution. Its volume was reduced to 1 mL by evaporation of H_2S at −60 °C, and the resulting yellow residue was cautiously dissolved by addition of 40 mL of CH_2Cl_2. A gentle stream of air was bubbled through the solution, whereupon its color rapidly turned to turquoise-green. While the mixture was stirred at room temperature for 10 h, a dark blue suspension formed, the volume of which was reduced to half. The microcrystalline product was filtered off, washed with 10 mL of CH_2Cl_2, and recrystallized from CH_2Cl_2/MeOH. Yield: 760 mg (72%). Anal. Calcd for $C_{65}Cl_2H_{56}P_2Ru_2S_{10}$ (1491.68): C, 52.34; H, 3.78; S, 21.50. Found: C, 52.61; H, 3.82; S, 21.40.

2·CS_2 from $[Ru(PPh_3)('S_4')]_x$. To a solution of $[Ru(PPh_3)('S_4')]_x$ (560 mg, 0.82 mmol) in 20 mL of CS_2 was added elemental sulfur (105 mg, 0.41 mmol). The color of the solution rapidly turned from red to dark green, and microcrystalline black-blue 2·CS_2 precipitated. After the mixture was stirred for another 10 h, 2·CS_2 was separated, washed with 30 mL of CS_2, and dried in vacuum for 1 day. Yield: 540 mg (89%). Anal. Calcd for $C_{65}H_{54}P_2Ru_2S_{12}$ (1484.03): C, 52.61; H, 3.67. Found: C, 52.30; H, 3.58.

$[\{Ru(PPh_3)\}(\mu\text{-}'S_4'CS_2)\{Ru(PPh_3)('S_4')\}]\cdot CS_2$ (3·CS_2) from $[Ru(PPh_3)('S_4')]_x$. From a clear red solution of $[Ru(PPh_3)('S_4')]_x$ (520 mg, 0.77 mmol) in 25 mL of CS_2, deep red 3·CS_2 precipitated within 3 h. It was filtered off, washed with 15 mL of CS_2, and dried in vacuum for 1 day. Yield: 510 mg (88%). Anal. Calcd for $C_{66}H_{54}P_2Ru_2S_{12}$ (1496.04): C, 52.30; H, 3.58; S, 25.72. Found: C, 51.88; H, 3.61; S, 24.95.

X-ray Structure Determinations. Yellow-orange cubes of **1**·THF were obtained from a saturated solution of freshly synthesized **1** in H_2S-saturated THF that was layered with the same volume of H_2S-saturated pentane for 3 days at 0 °C.

Single crystals of 2·CH_2Cl_2 could so far be obtained only when saturated solutions of **2** were layered with MeOH at −60 °C and subsequently slowly warmed to room temperature. After 2–3 weeks the turquoise-blue solutions and also the precipitated crystals started decomposing under decolorization. Accordingly, the single crystals that could be obtained were small and of poor quality, and the crystallographic data allowed solution of the structure of 2·CH_2Cl_2 but not a satisfactory refinement.

In the presence of air, very slow evaporation of deep red solutions of $[Ru(PPh_3)('S_4')]_x$ in CS_2 yielded black cubes of 2·CS_2. Deep red single crystals of 3·CS_2 were obtained from CS_2 solutions of $[Ru(PPh_3)('S_4')]_x$ that were stored in Schlenk tubes closed by rubber stoppers. In the course of ca. 14 days, the solvent evaporated through the rubber stoppers and the remaining crystals were separated and washed with ether/CH_2Cl_2 (3:1).

The single crystals of **1**·THF, 2·CH_2Cl_2, 2·CS_2, and 3·CS_2 were sealed under N_2 in glass capillaries. The structures were solved by direct methods (SHELXTL PLUS). Only in the case of 2·CH_2Cl_2 were the carbon atoms refined isotropically; in all other cases, non-hydrogen atoms were refined anisotropically. The aromatic hydrogen atoms were calculated for ideal geometry and restricted during refinement; the methyl hydrogen atoms were calculated for ideal tetrahedra and rotated around their central carbon atom during refinement; the isotropic hydrogen atoms were refined with common temperature factors. The H_2S hydrogen atoms of **1**·THF were located by difference Fourier synthesis and fixed during refinement. Due to inferior refinement, hydrogen atoms of 3·CS_2 were not calculated. Table I summarizes crystallographic data of the complexes.

Results

Synthesis and Characterization of $[Ru(SH_2)(PPh_3)('S_4')]$ (1), $[(\mu\text{-}S_2)\{Ru(PPh_3)('S_4')_2\}]$ (2), and $[\{Ru(PPh_3)\}(\mu\text{-}'S_4'CS_2)\{Ru(PPh_3)('S_4')\}]$ (3). Red $[Ru(PPh_3)('S_4')]_x$[11] formally contains a five-coordinate Ru center and reacts with thioethers or disulfides, e.g., SPh_2, SPhMe, SMe_2,[11] and CH_3SSCH_3,[12] in MeOH suspensions at room temperature (eq 1).

$$[Ru(PPh_3)('S_4')]_x + L \xrightarrow[rt]{MeOH} [Ru(L)(PPh_3)('S_4')] \quad (1)$$

L = monodentate sulfur ligand

The analogous H_2S complex, $[Ru(SH_2)(PPh_3)('S_4')]$ (**1**), could not be obtained under these conditions. According to eq 2 only a mixture of $[(\mu\text{-}S_2)\{Ru(PPh_3)('S_4')_2\}]$ (**2**)[2] and other noncharacterized compounds formed.

$$[Ru(PPh_3)('S_4')]_x + H_2S(g) \xrightarrow[rt/1\ day]{MeOH} \underset{\mathbf{2}}{[(\mu\text{-}S_2)\{Ru(PPh_3)('S_4')_2\}]} + \text{other compounds} \quad (2)$$

The synthesis of **1** finally succeeded in liquid H_2S at −70 °C according to eq 3.

$$[Ru(PPh_3)('S_4')]_x + H_2S(l) \xrightarrow[5\ min]{-70\ °C} \underset{\mathbf{1}}{[Ru(SH_2)(PPh_3)('S_4')]} \quad (3)$$

(12) Sellmann, D.; Lechner, P.; Moll, M. *Z. Naturforsch.* **1991**, *46b*, 1459.

Table II. Selected Spectroscopic Data for [Ru(SH$_2$)(PPh$_3$)'S$_4$']·THF (**1**·THF), [(μ-S$_2$){Ru(PPh$_3$)'S$_4$'}$_2$] (**2**), and [{Ru(PPh$_3$)}(μ-'S$_4$'CS$_2$){Ru(PPh$_3$)'S$_4$'}] (**3**)

compound	IR (KBr): ν, cm^{-1}	NMR:[a] δ, ppm		UV–vis–near-IR:[b] λ, nm (ϵ, 10^{-3} L mol^{-1} cm^{-1})	FD-MS: m/e
[Ru(SH$_2$)(PPh$_3$)'S$_4$']·THF	2410 ν(S–H···O) 2290 ν(S–H···S)	^{1}H	7.67–6.40 (23 H, m, C$_6$H$_4$, PPh$_3$)[c] 2.85–2.35 (4 H, m, C$_2$H$_4$) 1.96 (2 H, s, SH)		706
		^{31}P	42.2[c] 41.0[d]		
[Ru(SD$_2$)(PPh$_3$)'S$_4$']		^{1}H	8.00–6.30 (23 H, m, C$_6$H$_4$, PPh$_3$)[d] 2.32–1.59 (4 H, m, C$_2$H$_4$)		708
		^{31}P	41.0[d]		
[(μ-S$_2$){Ru(PPh$_3$)'S$_4$'}$_2$]	536[l]/525[m] ν(S–S)[h] 384[m]/372[l] ν(Ru–S)	^{1}H	7.64–6.63 (46 H, m, C$_6$H$_4$, PPh$_3$)[e] 3.97–2.14 (8 H, m, C$_2$H$_4$)	645 (0.9)[e,i] 1049 (13.7)	1408
		^{31}P	34.0[e,m] 34.4[m]/32.1[d,l]		
[{Ru(PPh$_3$)}(μ-'S$_4$'CS$_2$){Ru(PPh$_3$)'S$_4$'}]	1075 ν(C=S)	^{1}H	7.87–6.43 (46 H, m, C$_6$H$_4$, PPh$_3$)[f] 3.18–1.40 (8 H, m, C$_2$H$_4$)	510 (13.6)[e]	
		^{31}P	38.5/31.2[g,j] 38.7/33.4 38.5/30.8[e,k] 39.3/33.7		

[a] 270 MHz. [b] Solutions 1×10^{-4} M. [c] In CD$_2$Cl$_2$/THF-d_8 (1:2). [d] In C$_6$D$_6$. [e] In CD$_2$Cl$_2$. [f] In CS$_2$/CD$_2$Cl$_2$ (3:1). [g] In CS$_2$. [h] Resonance Raman spectrum at λ = 647.1 nm. [i] Identical for both diastereomers. [j] From reaction solution. [k] From the isolated substance. [l] Noncentrosymmetric *RR/SS* pair of enantiomers. [m] Centrosymmetric *RS* isomer.

Under an atmosphere of H_2S, **1** precipitates in yellow-orange crystals as **1**·THF on recrystallization from H_2S-saturated THF. In contrast to the highly labile solvent-free **1**, the solvated **1**·THF is stable at 25 °C, loses H_2S slowly in vacuum only, and can be ionized in the mass spectrometer without decomposition. **1** shows one single broad ν(SH) at 2300 cm^{-1} (KBr), whereas **1**·THF exhibits two ν(SH) at 2410 and 2290 cm^{-1}.

^{1}H NMR spectroscopic evidence for SH protons in **1** is obtained only with solutions of freshly prepared **1** in H_2S-containing mixtures of CD_2Cl_2/THF-d_8 (1:2). They exhibit the signal of free H_2S (δ = 1.00 ppm) and, in addition, the slightly broadened signal for the protons of the H_2S ligand at δ = 1.96 ppm. The ^{1}H NMR spectrum of the corresponding D_2S complex [Ru(SD$_2$)(PPh$_3$)'S$_4$'] does not show such a resonance.[13] When the sample is slowly oxidized by air, the signal for the H_2S ligand decreases and simultaneously splits into two signals, until it finally disappears. The splitting may be traced to the intermediate formation of two diastereomers of the μ-S_2H_2 complex [(μ-S_2H_2){Ru(PPh$_3$)'S$_4$'}$_2$] that, however, could not be isolated or further characterized. The final product is always turquoise-blue [(μ-S$_2$){Ru(PPh$_3$)'S$_4$'}$_2$] (**2**) (eq 4). **2** is also obtained when both **1** and **1**·THF are oxidized in the solid state by O_2.

$$2[\underset{\mathbf{1}}{Ru(SH_2)(PPh_3)'S_4'}] \xrightarrow[-2H_2O]{+O_2} [\underset{\mathbf{2}}{(\mu\text{-}S_2)\{Ru(PPh_3)'S_4'\}_2}] \quad (4)$$

We recently reported syntheses for **2** using S_8 and NBu_4SH as the sources of S_2 units;[2] oxidation of **1** is another possibility to obtain **2**, whose formation is easily observed due to its characteristic color. **2** was further identified by ^{31}P{^{1}H} NMR spectra. Two signals at 34.4 and 32.1 ppm (C_6D_6) in the spectra of **2**, formed according to eq 4, showed that **2** can exist in two diastereomeric forms (see below).

Also CS_2 can act as source of S_2 units. We observed this when we attempted to obtain single crystals of the so far only unsatisfactorily characterized [Ru(PPh$_3$)'S$_4$']$_x$ by recrystallizing it from CS_2. Single crystals of [Ru(PPh$_3$)'S$_4$']$_x$ were not obtained, but in the presence of air slow evaporation of the solvent yielded black crystals of **2**·CS_2 (eq 5).

$$[Ru(PPh_3)'S_4']_x \xrightarrow[\text{rt/2–3 days}]{CS_2/O_2} \mathbf{2}\cdot CS_2 + \text{other products} \quad (5)$$

It remains uncertain so far whether **2** is formed by direct addition of sulfur originating from oxidation of CS_2 or by oxidation of the binuclear thioxanthate complex [{Ru(PPh$_3$)}(μ-'S$_4$'CS$_2$)-{Ru(PPh$_3$)'S$_4$'}] (**3**).

Dissolution of [Ru(PPh$_3$)'S$_4$']$_x$ in CS_2 yields deep red solutions. They do not contain [Ru(PPh$_3$)'S$_4$']$_x$, but deep red **3** (λ_{max} = 510 nm) formed according to eq 6 by addition of CS_2 to mononuclear [Ru(PPh$_3$)'S$_4$'] fragments.

$$2[Ru(PPh_3)(S_4)] + CS_2 \xrightarrow[\text{rt/3 h}]{CS_2} \quad (6)$$

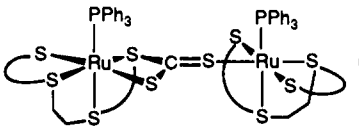

3

It is to be expected that formation of **3** from racemic [Ru(PPh$_3$)'S$_4$'] fragments leads to two diastereomeric pairs of enantiomers (see below). They give rise to four signals in the ^{31}P{^{1}H} NMR spectrum of the reaction solution (Figure 1) that exhibit approximately pairwise equal intensities. One pair of enantiomers of **3** could be isolated from these solutions as **3**·CS_2 and characterized by X-ray crystallography.

The addition of CS_2 to [Ru(PPh$_3$)'S$_4$'] fragments according to eq 6 is likely reversible because addition of elemental sulfur to the CS_2 solutions leads again to rapid formation of the μ-S_2 complex **2** (eq 7).

$$[Ru(PPh_3)'S_4']_x + S_8 \xrightarrow[\text{rt/10 h}]{CS_2} \underset{\mathbf{2}\cdot CS_2}{[(\mu\text{-}S_2)\{Ru(PPh_3)'S_4'\}_2]\cdot CS_2} \quad (7)$$

Table II is a listing of selected spectroscopic data of **1**–**3**.

X-ray Structure Determinations. The molecular structures of **1**·THF (Figure 2a), **2**·CH_2Cl_2 (Figure 3a), **2**·CS_2 (Figure 3b), and **3**·CS_2 (Figure 4) were determined by X-ray crystallography. **2**·CH_2Cl_2 and **2**·CS_2 contain diastereomeric forms of **2**. For this reason, the structure of **2**·CH_2Cl_2 will be included although its refinement stopped at an unsatisfactory R = 0.151, not allowing discussion of bond distances and angles. Table III lists selected distances and angles of the complexes.

In all complexes the Ru atoms are found in sulfur-dominated coordination spheres. The Ru centers are pseudooctahedrally coordinated by one phosphorus and five sulfur donors; angles as well as Ru–S and Ru–P distances within the coordination polyhedra show no anomalies.

In the unit cell of **1**·THF, enantiomers of **1** are associated via two S–H···S bridges to give a cyclic centrosymmetric dimer. In addition, a THF molecule is bound to each H_2S ligand via one S–H···O bridge (Figure 2b).

(13) The D_2S required for the synthesis of [Ru(SD$_2$)(PPh$_3$)'S$_4$'] was prepared from Na_2S and D_2SO_4 (50% in D_2O), condensed into a Schlenk tube at −78 °C, and dried over 4-Å molecular sieves.

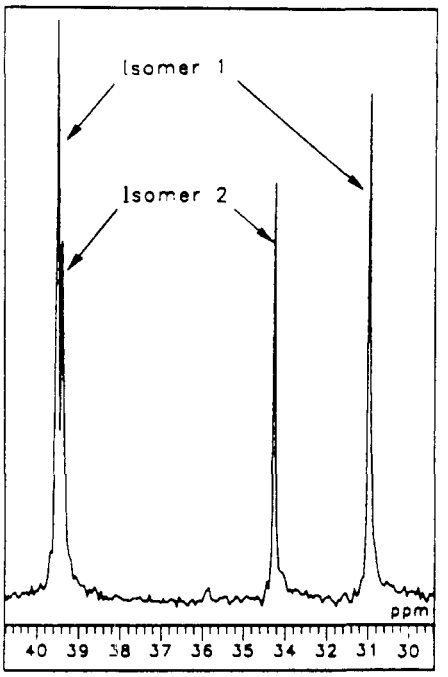

Figure 1. $^{31}P\{^1H\}$ NMR spectrum of the deep red solution of **3** in CS_2.

The S–H···S bridges in **1**·THF (Figure 5) form angles of 153°; the sum of the distances S(5)–H(5A) and H(5A)···S(4A) is 378 pm and the distance S(5)···S(4A) is 369 pm. The S–H···O bridges possess angles of 159°, and the S···O distance is 333 pm. The very short S···S and S···O distances indicate that these hydrogen bridges must be strong.

The Ru(1)–S(3) distance (229.3 (5) pm) in **1**·THF in trans position to the H_2S ligand is distinctly shorter than the other Ru–S distances (236.1 (5)–239.7 (5) pm); comparison with related $[Ru(L)(PPh_3)'S_4']$ complexes[14] suggests that this effect is due to a strong Ru→S(thioether) π-acceptor bond.

The structure of **2**·CH_2Cl_2 (Figure 3b) could be solved but, as mentioned above, not satisfactorily refined. In **2**·CH_2Cl_2, two enantiochiral $[Ru(PPh_3)'S_4']$ fragments are centrosymmetrically bridged via the η^1-η^1-S_2 ligand; the inversion center is located in the middle of the μ-S_2 unit. The RuSSRu core forms a plane toward which the $[Ru(PPh_3)'S_4']$ fragments are slightly twisted such that the Ru–P bonds form an angle of 47° with the RuSSRu plane. Both $[Ru(PPh_3)'S_4']$ fragments are eclipsed; the Ru–P bonds lie in a plane and stand in trans position with regard to the RuSSRu plane.

The structure of **2**·CS_2 could be fully refined (Figure 3b). In **2**·CS_2, the η^1–η^1-S_2 ligand bridges two $[Ru(PPh_3)'S_4']$ fragments that are formally homochiral; distances and angles in both fragments, however, are slightly different. Accordingly, the whole molecule has C_1 symmetry only. The $[Ru(PPh_3)'S_4']$ fragments are somewhat gauche configurated; the Ru–P bonds include an angle of 23° and accept cisoid positions with regard to the RuSSRu plane. The RuSSRu core has again trans configuration; it is, however, not exactly planar, and the Ru(1)–S(5) and Ru(2)–S(10) bonds form a dihedral angle of 5.1°.

The S–S distance of 199.1 (4) pm[15] is relatively short and lies between the values of free S_2 (188.7 pm)[3a] and H_2S_2 (205.5 pm)[16] such that partial double-bond character for the μ-S_2 unit is indicated. Other μ-S_2 complexes usually show longer S–S distances between 201 and 205 pm,[3] and a shorter S–S distance than in **2**·CS_2 has been found only in $[(\mu\text{-}S_2)\{Ru(Cp)(PMe_3)_2\}_2](BF_4)_2$ (196.2 (4) pm).[8] Typical S–S single bonds, e.g., in organic disulfides, exhibit lengths of ca. 210 pm.[17]

Table III. Selected Interatomic Distances (pm) and Angles (deg) for **1**·THF, **2**·CS_2, and **3**·CS_2

	$[Ru(SH_2)(PPh_3)'S_4']$·THF (**1**·THF)		
Ru(1)–S(1)	239.7 (5)	S(5)–H(5A)	119
Ru(1)–S(2)	236.1 (5)	S(5)–H(5B)	121
Ru(1)–S(3)	229.3 (5)	H(5A)···S(4A)	258
Ru(1)–S(4)	239.3 (5)	H(5B)···O(1)	216
Ru(1)–S(5)	239.9 (5)	S(5)···S(4A)	369
Ru(1)–P(1)	232.4 (5)		
S(1)–Ru(1)–S(2)	86.2 (1)	S(1)–Ru(1)–P(1)	97.7 (1)
S(1)–Ru(1)–S(3)	88.0 (1)	S(2)–Ru(1)–P(1)	174.8 (1)
S(1)–Ru(1)–S(4)	171.3 (1)	S(3)–Ru(1)–P(1)	95.4 (1)
S(1)–Ru(1)–S(5)	87.4 (1)	S(4)–Ru(1)–P(1)	89.6 (1)
S(2)–Ru(1)–S(3)	88.2 (1)	S(5)–Ru(1)–P(1)	88.9 (1)
S(2)–Ru(1)–S(4)	86.8 (1)	Ru(1)–S(5)–H(5A)	102
S(2)–Ru(1)–S(5)	87.9 (1)	Ru(1)–S(5)–H(5B)	121
S(3)–Ru(1)–S(4)	86.6 (1)	H(5A)–S(5)–H(5B)	77
S(3)–Ru(1)–S(5)	174.1 (1)	S(5)–H(5A)–S(4A)	153
S(4)–Ru(1)–S(5)	97.6 (1)	Ru(1)–S(4)–H(5AA)	129
		S(5)–H(5B)–O(1)	159
	$[(\mu\text{-}S_2)\{Ru(PPh_3)'S_4'\}_2]$·$CS_2$ (**2**·CS_2)		
Ru(1)–S(1)	235.7 (3)	Ru(2)–S(6)	236.0 (3)
Ru(1)–S(2)	236.5 (3)	Ru(2)–S(7)	236.2 (3)
Ru(1)–S(3)	239.1 (3)	Ru(2)–S(8)	239.8 (3)
Ru(1)–S(4)	242.1 (3)	Ru(2)–S(9)	242.0 (3)
Ru(1)–S(5)	224.5 (3)	Ru(2)–S(10)	224.2 (3)
Ru(1)–P(1)	234.1 (3)	Ru(2)–P(2)	235.2 (3)
S(5)–S(10)	199.1 (4)	S(4)···S(12)	355
		S(5)···S(11)	385
S(1)–Ru(1)–S(2)	86.9 (1)	S(6)–Ru(2)–S(7)	87.1 (1)
S(1)–Ru(1)–S(3)	87.5 (1)	S(6)–Ru(2)–S(8)	86.6 (1)
S(1)–Ru(1)–S(4)	169.3 (1)	S(6)–Ru(2)–S(9)	170.1 (1)
S(1)–Ru(1)–S(5)	93.0 (1)	S(6)–Ru(2)–S(10)	95.7 (1)
S(2)–Ru(1)–S(3)	86.9 (1)	S(7)–Ru(2)–S(8)	86.4 (1)
S(2)–Ru(1)–S(4)	86.2 (1)	S(7)–Ru(2)–S(9)	87.0 (1)
S(2)–Ru(1)–S(5)	92.2 (1)	S(7)–Ru(2)–S(10)	91.9 (1)
S(3)–Ru(1)–S(4)	84.0 (1)	S(8)–Ru(2)–S(9)	85.1 (1)
S(3)–Ru(1)–S(5)	179.0 (1)	S(8)–Ru(2)–S(10)	177.0 (1)
S(4)–Ru(1)–S(5)	95.4 (1)	S(9)–Ru(2)–S(10)	92.3 (1)
S(1)–Ru(1)–P(1)	93.8 (1)	S(6)–Ru(2)–P(2)	92.7 (1)
S(2)–Ru(1)–P(1)	179.4 (1)	S(7)–Ru(2)–P(2)	178.7 (1)
S(3)–Ru(1)–P(1)	93.0 (1)	S(8)–Ru(2)–P(2)	92.3 (1)
S(4)–Ru(1)–P(1)	93.2 (1)	S(9)–Ru(2)–P(2)	93.0 (1)
S(5)–Ru(1)–P(1)	87.9 (1)	S(10)–Ru(2)–P(2)	89.4 (1)
Ru(1)–S(5)–S(10)	110.3 (1)	Ru(2)–S(10)–S(5)	111.4 (1)
	$[\{Ru(PPh_3)\}(\mu\text{-}'S_4'CS_2)\{Ru(PPh_3)'S_4'\}]$·$CS_2$ (**3**·CS_2)		
Ru(1)–S(1)	239.6 (8)	Ru(2)–S(6)	239.2 (8)
Ru(1)–S(2)	232.7 (8)	Ru(2)–S(7)	230.0 (9)
Ru(1)–S(3)	236.0 (6)	Ru(2)–S(8)	240.0 (7)
Ru(1)–S(4)	240.0 (7)	Ru(2)–S(9)	235.0 (9)
Ru(1)–S(5)	236.3 (9)	Ru(2)–S(10)	244.6 (9)
Ru(1)–P(1)	234.2 (6)	Ru(2)–P(2)	234.1 (8)
C(1)–S(5)	159.3 (30)	C(1)–S(9)	189.1 (28)
		C(1)–S(10)	173.4 (26)
S(1)–Ru(1)–S(2)	87.4 (3)	S(6)–Ru(2)–S(7)	86.4 (3)
S(1)–Ru(1)–S(3)	85.8 (2)	S(6)–Ru(2)–S(8)	84.9 (3)
S(1)–Ru(1)–S(4)	169.4 (3)	S(6)–Ru(2)–S(9)	170.0 (3)
S(1)–Ru(1)–S(5)	105.4 (3)	S(6)–Ru(2)–S(10)	102.1 (3)
S(2)–Ru(1)–S(3)	87.8 (3)	S(7)–Ru(2)–S(8)	88.0 (3)
S(2)–Ru(1)–S(4)	84.9 (3)	S(7)–Ru(2)–S(9)	98.5 (3)
S(2)–Ru(1)–S(5)	164.9 (3)	S(7)–Ru(2)–S(10)	170.9 (3)
S(3)–Ru(1)–S(4)	86.8 (2)	S(8)–Ru(2)–S(9)	86.5 (3)
S(3)–Ru(1)–S(5)	85.1 (3)	S(8)–Ru(2)–S(10)	89.6 (3)
S(4)–Ru(1)–S(5)	81.4 (3)	S(9)–Ru(2)–S(10)	72.6 (3)
S(1)–Ru(1)–P(1)	92.4 (2)	S(6)–Ru(2)–P(2)	94.8 (3)
S(2)–Ru(1)–P(1)	90.7 (3)	S(7)–Ru(2)–P(2)	91.6 (3)
S(3)–Ru(1)–P(1)	177.7 (3)	S(8)–Ru(2)–P(2)	179.5 (4)
S(4)–Ru(1)–P(1)	94.9 (2)	S(9)–Ru(2)–P(2)	93.8 (3)
S(5)–Ru(1)–P(1)	96.6 (3)	S(10)–Ru(2)–P(2)	90.7 (3)
Ru(1)–S(5)–C(1)	123.9 (10)	Ru(2)–S(9)–C(1)	91.6 (9)
S(5)–C(1)–S(9)	114.9 (13)	Ru(2)–S(10)–C(1)	92.5 (10)
S(5)–C(1)–S(10)	141.8 (17)		
S(9)–C(1)–S(10)	103.1 (15)		

(14) Sellmann, D.; Barth, I.; Knoch, F.; Moll, M. *Inorg. Chem.* **1990**, *29*, 1822 and literature reported therein.

(15) The S–S distances of the *RS* and *SR* isomers of **2** in **2**·CH_2Cl_2 also lie in this area. But owing to the insufficient refinement of crystallographic data, exact statements about the S–S distances cannot be made.

(16) Winnewisser, G.; Winnewisser, H.; Gordy, W. *J. Chem. Phys.* **1968**, *49*, 3465.

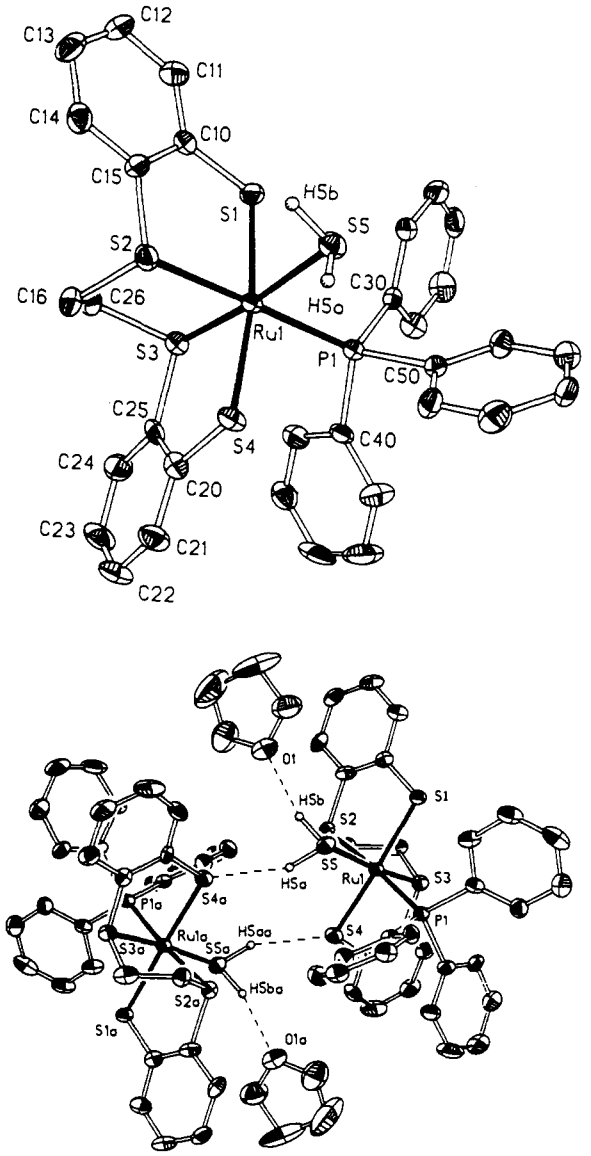

Figure 2. (a, top) Molecular structure of 1·THF (THF and H atoms omitted except of H(5A) and H(5B)). (b, bottom) Association of enantiomers via S–H···S bridges.

Double-bond character is also indicated for the Ru–S bonds within the RuSSRu core. They are clearly shorter (224.2 (3), 225.5 (3) pm) than the remaining Ru–S distances (235.7 (3)–242.1 (3) pm).

The slightly different angles and distances within both formally homochiral [Ru(PPh$_3$)'S$_4$'] fragments and the distortion of the RuSSRu core are presumably caused by packing effects as well as interactions between the CS$_2$ solvate and one of both [Ru(PPh$_3$)'S$_4$'] fragments (Figure 6a). The distance between the thiolate atom S(4) of the more strongly distorted [Ru(PPh$_3$)'S$_4$'] fragment and the sulfur atom S(12) of the CS$_2$ solvate is shorter (355 pm) than the sum of van der Waals radii (370 pm) and indicates attractive S···S interactions. Such van der Waals contacts between nonbonded sulfur atoms were also found, e.g., in α- and β-H_2CS_3.[18]

In 3, two formally homochiral [Ru(PPh$_3$)'S$_4$'] fragments are connected by a CS$_2$ unit. Addition of CS$_2$ to a thiolate S atom of the 'S$_4$' ligand in [Ru(PPh$_3$)'S$_4$'] yields a thioxanthate ligand.

(17) (a) van Wart, H. E.; Sheraga, H. A. *J. Phys. Chem.* **1976**, *80*, 1823. (b) Steudel, R. *Angew. Chem.* **1975**, *87*, 683; *Angew. Chem., Int. Ed. Engl.* **1975**, *14*, 655.

(18) (a) Krebs, B.; Henkel, G.; Dinglinger, H. J.; Stehmeier, G. *Z. Kristallogr.* **1980**, *153*, 285. (b) Krebs, B.; Henkel, G. *Z. Kristallogr.* **1987**, *179*, 373.

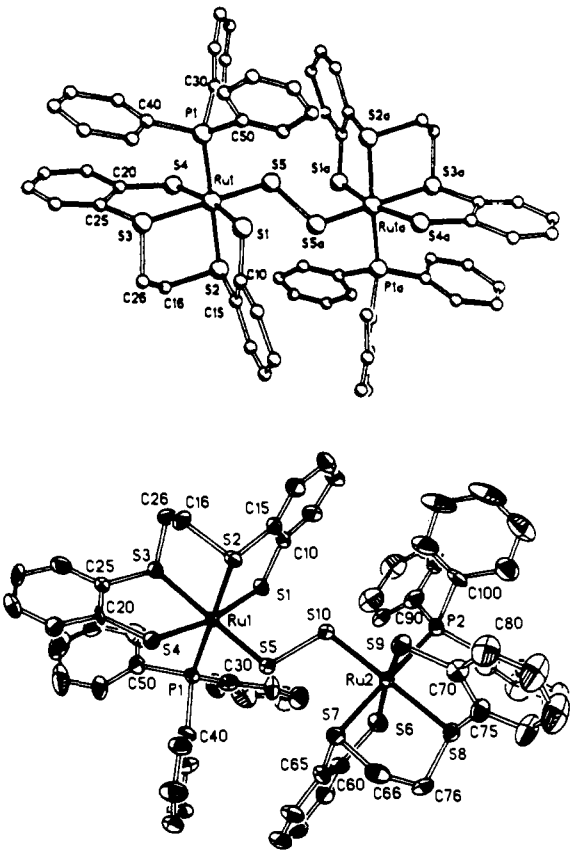

Figure 3. Molecular structures of (a, top) 2·CH_2Cl_2 and (b, bottom) 2·CS_2 (H atoms and solvent omitted).

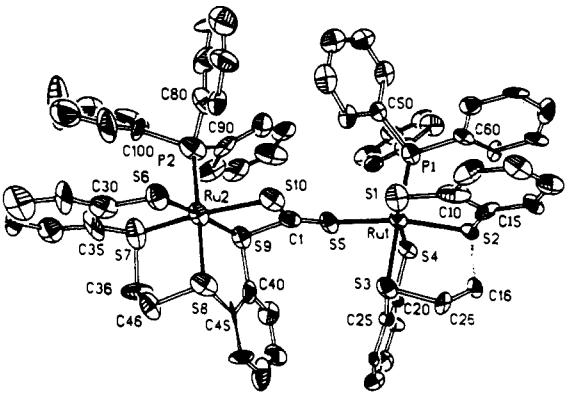

Figure 4. Molecular structure of 3·CS_2 (H atoms and solvent omitted).

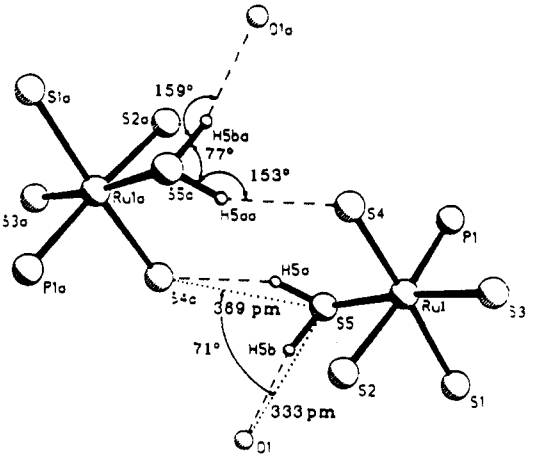

Figure 5. S–H···S and S–H···O hydrogen bridges in 1·THF.

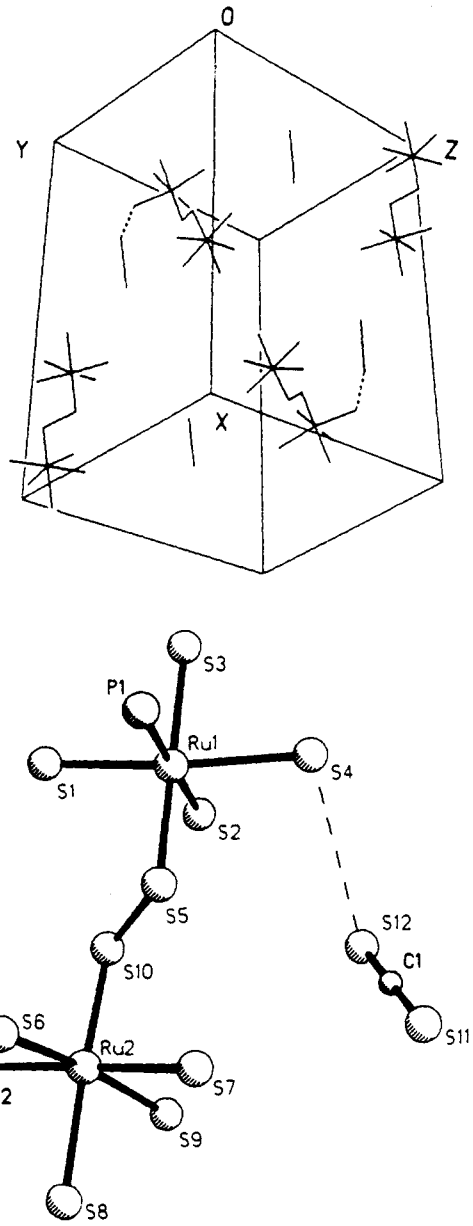

Figure 6. (a, top) Packing of $2 \cdot CS_2$ in the unit cell and (b, bottom) interaction between the thiolate donor S(4) and CS_2.

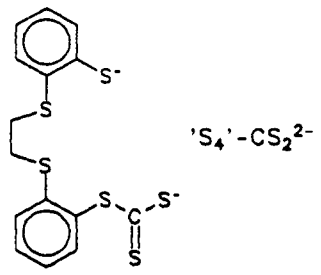

Figure 7. Thioxanthate ligand 'S_4'CS_2^{2-}.

This is to be concluded from angles and distances within the 'S_4'CS_2 ligand (Figure 7).

The C(1)–S(5) bond length (159.3 (30) pm) is appreciably shorter than the C(1)–S(9) (189.1 (28) pm) and C(1)–S(10) bonds (173.4 (26) pm) and indicates distinct double-bond character. The C(1)–S(5)–Ru(1) angle is 123.9 (10)°; the distance Ru(1)–S(5) (236.3 (9) pm) is comparable with the other Ru–S distances.

In **3**, the 'S_4'CS_2^{2-} ligand coordinates one Ru center via two thiolate and three thioether donors and the second Ru center via the remaining thiocarbonyl function S(5).

Scheme I. Potential Stereoisomers of Binuclear $[(\mu\text{-L})\{Ru(PPh_3)'S_4'\}_2]$ Complexes with Bridging Ligands L = S_2 or CS_2

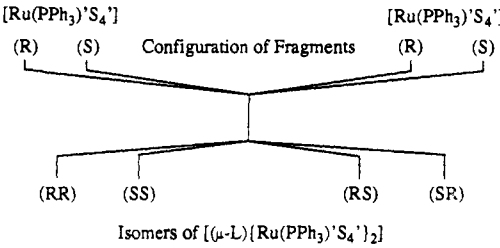

Discussion

S–H···S Hydrogen Bridges in 1·THF. $[Ru(SH_2)(PPh_3)'S_4']\cdot$THF (**1**·THF) is the first example of the rare H_2S complexes that could be completely characterized not only by spectroscopic means but also by X-ray structure determination.

The S–H···S bridges are of particular interest. For the first time the existence of these bridges in H_2S complexes could be proved by X-ray crystallography. Unlike common S–H···S bridges, e.g., in H_2S (ΔH_f^{298} = 7 kJ mol^{-1})[19] that are usually weak, the bridges in **1**·THF have got to be very strong, which follows from their properties.

The strongest S–H···S bridges hitherto known ($\Delta H_f^{298} \approx 12$ kJ mol^{-1})[20] were found in dithiophosphinic acids, which have S···S distances of 375–384 pm, ν(SH) between 2340 and 2400 cm^{-1} (KBr), and S–H···S angles in the range 159–173°.[21] Compared with this, the calculated S–H···S limiting distance is ca. 439 pm[22] and the ν(SH) frequencies in gaseous H_2S occur at 2615 and 2628 cm^{-1}.[23]

In comparison, the S···S distances in the S–H···S bridges of **1**·THF are only 369 pm, and in particular, these extremely short distances indicate that the S–H···S bridges are exceptionally strong. This indication is corroborated by the ν(S–H···S) at 2290 cm^{-1} (KBr). It is the lowest frequency so far observed for S–H···S bridges. In H_2S complexes that form no hydrogen bridges, the ν(SH) appear at significantly higher wavenumbers (2590–2510 cm^{-1}).[4a-e]

In contrast to **1**, **1**·THF shows also a ν(S–H···O) at 2410 cm^{-1} in the IR spectrum (KBr). This frequency as well as the short S···O distance also suggests that the S–H···O bridges are strong.[24]

Stereoisomerism of 2 and 3. When binuclear complexes form from racemates of *R*- and *S*-configurated $[Ru(PPh_3)'S_4']$ fragments, *RR*, *SS*, *RS*, and *SR* combinations are to be expected, but the number of actually resulting stereoisomers depends on the nature of the linkage. For example, 10 different stereoisomers are possible by direct linkage of the fragments via thiolate atoms of the 'S_4' ligands.[25]

If *R* and *S* fragments are bridged by a S_2 unit as in **2**, and if both fragments can freely rotate with regard to each other, only four isomers are expected in accordance with Scheme I. In this case, the *RR* and *SS* isomers exist as pair of enantiomers, whereas the *RS* and *SR* isomers are identical.

C_i is the highest possible symmetry expected for the *RS* isomer and C_2 symmetry for the *RR*/*SS* diasteromers. Both diastereomeric forms of **2** each should cause only one signal in the $^{31}P\{^1H\}$ NMR spectrum.

Scheme I is also valid for **3**. In this case, however, the *RS* and *SR* isomers are not centrosymmetric and form a pair of enan-

(19) Singh, S.; Rao, C. N. R. *J. Phys. Chem.* **1967**, *71*, 1074.
(20) Shagidullin, R. R.; Lipatova, I. P.; Vachugova, L. I.; Cherkasov, R. A.; Khairutdinova, F. K. *Izv. Akad. Nauk SSSR Ser. Khim.* **1972**, 847.
(21) (a) Krebs, B. *Angew. Chem.* **1983**, *95*, 113; *Angew. Chem., Int. Ed. Engl.* **1983**, *22*, 113. (b) Krebs, B.; Henkel, G. *Z. Kristallogr.* **1987**, *179*, 373.
(22) In regard to S–H···S bridges, the sum of the van der Waals radii of sulfur (r_S) results in a completely insufficient value. Here the sum d_{S-H} (134 pm) + r_H (120 pm) + r_S (185 pm) has to be taken.[21a]
(23) Allen, H. C., Jr.; Blaine, L. R.; Plyler, E. K. *J. Chem. Phys.* **1956**, *24*, 35.
(24) Amos, R. D. *Chem. Phys.* **1986**, *104*, 145.
(25) (a) Sellmann, D.; Weiss, R.; Knoch, F. *Angew. Chem.* **1989**, *101*, 1719; *Angew. Chem., Int. Ed. Engl.* **1989**, *28*, 1703. (b) Sellmann, D.; Weiss, R.; Knoch, F.; Ritter, J. Dengler, G. *Inorg. Chem.* **1990**, *29*, 4107.

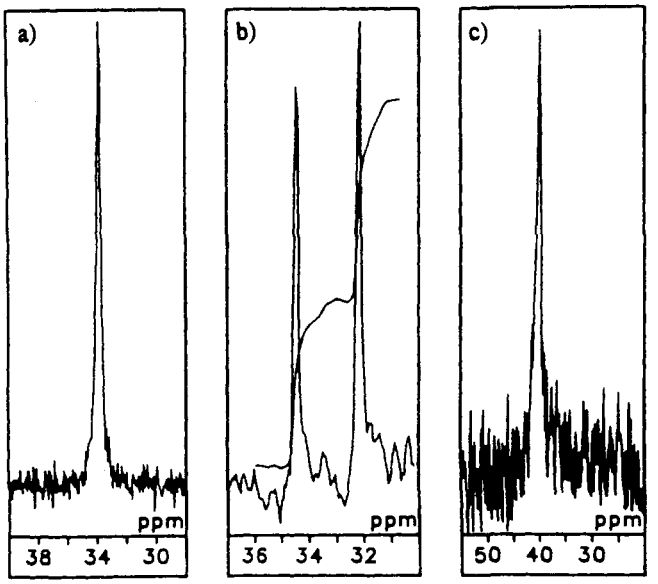

Figure 8. $^{31}P\{^1H\}$ NMR spectra of (a) centrosymmetric **2** (CD_2Cl_2), (b) the mixture of diastereomers of **2** obtained by the oxidation of **1** (C_6D_6), and (c) **1** (C_6D_6).

tiomers. The resulting two diastereomeric pairs of enantiomers of **3**, *RR/SS* and *RS/SR*, each are expected to give rise to two signals in the $^{31}P\{^1H\}$ NMR spectrum. As shown by the four signals in the spectrum of Figure 1, in fact both diastereomeric forms can be observed in solution during formation of **3** according to eq 6.

Spectra, Magnetism, and Bonding of 2. Analysis of $^{31}P\{^1H\}$ NMR spectra shows that the resulting ratio of diastereomers of **2** strongly depends on the specific synthetic route. When **2** formed according to eq 8,[2] the product showed only one single $^{31}P\{^1H\}$

$$rac\text{-}[Ru(PPh_3)'S_4']_x \xrightarrow[rt/1\ day]{THF/+S_8} \underset{\mathbf{2}}{[(\mu\text{-}S_2)\{Ru(PPh_3)'S_4'\}_2]} \quad (8)$$

NMR signal at 34.0 ppm (CD_2Cl_2) (Figure 8a) and could consequently contain only one of both possible diastereomers. X-ray crystallography of **2**·CH_2Cl_2 showed it to be the centrosymmetric *RS* isomer.

Oxidation of $[Ru(SH_2)(PPh_3)'S_4']$ (**1**) according to eq 4 leads to formation of both diastereomers of **2** in nearly equal amounts. The $^{31}P\{^1H\}$ NMR spectrum (C_6D_6) (Figure 8b) of the product exhibits two signals at 34.4 and 32.1 ppm. Due to its shift, the signal at 34.4 ppm can be assigned to the centrosymmetric *RS* isomer of **2**, and consequently, the second singlet at 32.1 ppm is to be assigned to the *RR/SS* pair of enantiomers of **2** that must possess C_2 symmetry. The diastereomers of **2** could not yet be separated by fractional crystallization. From CH_2Cl_2, they always crystallize as a mixture of diastereomers, and their low solubility prevented separation by chromatography.

The noncentrosymmetric *RR/SS* enantiomers were characterized in the X-ray structure determination of **2**·CS_2. All efforts to dissolve solid **2**·CS_2 in common solvents failed, and **2**·CS_2 could not be investigated by NMR spectroscopy. Distortion of the $[Ru(PPh_3)'S_4']$ fragments in solid **2**·CS_2 causes symmetry reduction of **2** from C_2 to C_1, but it may be fairly safely assumed that this reduction of symmetry is due to solid-state packing effects and that in solution the *RR/SS* enantiomers have C_2 symmetry.

Both diastereomers of **2** also exhibit different ν(S–S) and ν(Ru–S) frequencies for the RuSSRu core. Figure 9 shows the resonance Raman spectrum (λ_{exc} = 647.1 nm) of solid **2**·CH_2Cl_2 that, according to the $^{31}P\{^1H\}$ NMR spectra, contained centrosymmetric and noncentrosymmetric diastereomers of **2** in the ratio 4:1. In the respective regions, two pairs of bands appear at 536/525 and 384/372 cm^{-1}, which are assigned to ν(S–S) and ν(Ru–S) vibrations.

Due to their intensity, we assign the strong bands at 525 and 384 cm^{-1} to the centrosymmetric *RS* isomer and the weaker bands

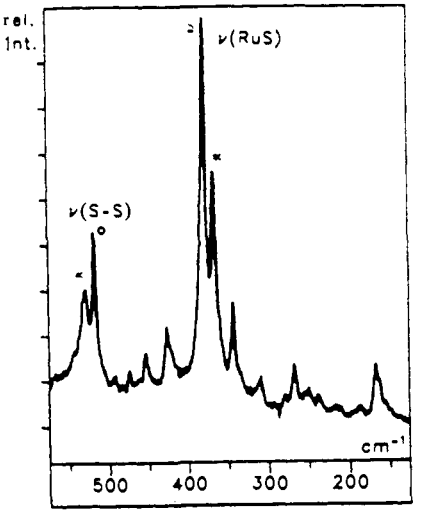

Figure 9. Resonance Raman spectrum (λ_{exc} = 647.1 nm) of the mixture of diastereomers (4:1) of **2**·CH_2Cl_2: *, *RS* isomer; o, *RR/SS* pair of enantiomers.

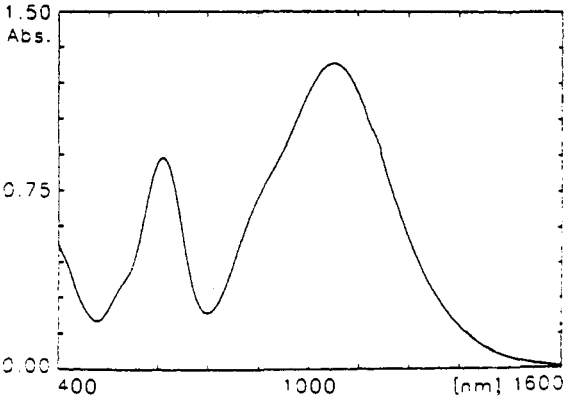

Figure 10. Electronic spectrum of **2** in CH_2Cl_2.

at 536 and 372 cm^{-1} to the *RR/SS* pair of enantiomers of **2**. Weak bands below 350 cm^{-1} can be assigned to ν(Ru–$S_{thiolate}$) and ν(Ru–$S_{thioether}$) vibrations within the $[Ru(PPh_3)'S_4']$ fragments.

The originally reported synthesis of **2** according to eq 8 always yielded products that exhibit a weak paramagnetism (μ_{eff} = 0.34 μ_B).[2] In this regard, **2** resembled $[(\mu\text{-}S_2)\{Ru(NH_3)_5\}_2]Cl_4$ which also possesses a small magnetic moment in spite of its even number of electrons.[5a,c] The weak paramagnetism of **2** gave rise to the question whether the unusual intensive band at 1049 nm (ϵ = 13 661 L mol^{-1} cm^{-1}) in the electronic spectrum of **2** (Figure 10) was due to intervalence charge transfer (ICT).

As described above, unsolvated **2** as well as both solvates **2**·CH_2Cl_2 and **2**·CS_2 could now be isolated in diamagnetic state. Hence, the weak paramagnetism of previously isolated **2** is certainly to be attributed to the presence of paramagnetic impurities.

The diamagnetic forms of **2** that could now be isolated, however, also exhibit the intense near-IR absorption at 1049 nm. It requires a discussion because for other μ-S_2 complexes a band in this region was not reported.

The deep turquoise-blue color of **2** indicates that the RuSSRu entity is a chromophore. It may be described by a delocalized 4c–6e π system as the related chromophores in, e.g., $[(\mu\text{-}N_2H_2)\{X\}_2]$ (X = $[CpMn(CO)_2]$, $[Cr(CO)_5]$, $[Ru(PPh_3)'S_4']$)[26] or $[(\mu\text{-}S_2)\{Y\}_2]^{n+}$ (Y = $[Ru(NH_3)_5]$, n = 4; $[CpRu(PMe_3)_2]$, n = 2).[5,8] Two occupied ruthenium d orbitals and the occupied π as well as the empty π^* orbital of the S_2 ligand combine to give one empty and three occupied molecular π orbitals (Figure 11). Energies and separation of these orbitals may be influenced by

(26) Sellmann, D.; Böhlen, E.; Waeber, M.; Huttner, G.; Zsolnai, L. *Angew. Chem.* **1985**, *97*, 984; *Angew. Chem., Int. Ed. Engl.* **1985**, *24*, 981 and literature reported therein.

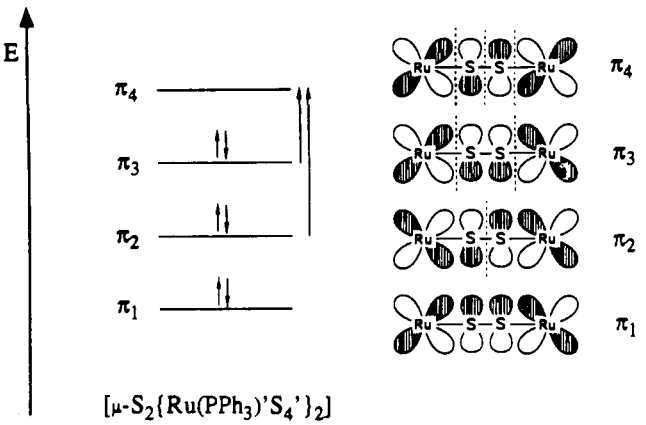

Figure 11. 4c–6e π system of the RuSSRu core in $[(\mu\text{-}S_2)\{Ru(PPh_3)\text{-}'S_4'\}_2]$ (**2**).

the coligands in various μ-S_2 complexes and may explain the different electronic spectra of, for instance, $[(\mu\text{-}S_2)\{Ru(NH_3)_5\}_2]^{4+}$ and $[(\mu\text{-}S_2)\{Ru(PPh_3)'S_4'\}_2]$ (**2**).

Thus, the intense green of $[(\mu\text{-}S_2)\{Ru(NH_3)_5\}_2]^{4+}$ (λ_{max} = 715 nm; ϵ = 14 900 L mol^{-1} cm^{-1}) can plausibly be attributed to the HOMO–LUMO transition $\pi_3 \rightarrow \pi_4$.[5] Transitions at longer wavelengths were not reported.[5]

In **2**, the electron-rich thiolate and thioether coligands may not only destabilize all π orbitals but also reduce the energy gaps between them. The HOMO–LUMO transition $\pi_3 \rightarrow \pi_4$ again causes the absorption at the longest wavelength that now, however, no longer appears in the visible but in the near-IR region at 1049 nm (ϵ = 13 661 L mol^{-1} cm^{-1}). Consequently, the intense color of **2** must be due to the $\pi_2 \rightarrow \pi_4$ transition giving rise to the band at 645 nm (ϵ = 8969 L mol^{-1} cm^{-1}). It appears at a slightly higher frequency than the $\pi_3 \rightarrow \pi_4$ band of $[(\mu\text{-}S_2)\{Ru(NH_3)_5\}_2]^{4+}$, and it is noteworthy that it has a distinctly lower intensity. This description of the RuSSRu core of **2** as a 4c–6e π system is supported by the bond distances found for **2**·CS_2.

Formation, Bonding, and Isomerism of 3. Formation of thioxanthate ligands Ia by insertion of CS_2 into metal–thiolate bonds is formally analogous to formation of carbonate ligands Ib by insertion of CO_2 into metal alkoxide bonds.[27]

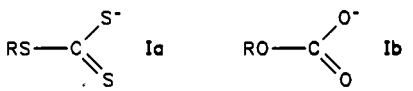

All sulfur atoms of the thioxanthate ligand can act as donors for metals, but out of the potentially resulting complexes IIa–IIIb,

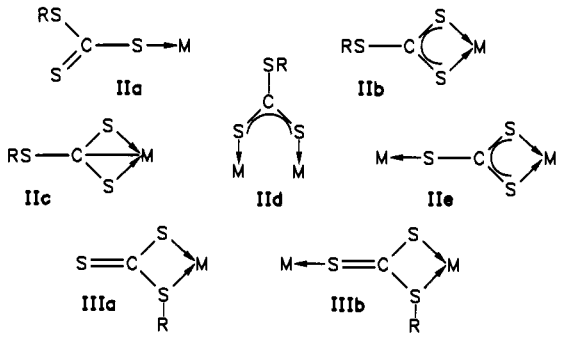

only types IIa–e were known so far.[27,28] IIb seems to be the most common bonding mode whereas IIe could be observed only with the CS_3^{2-} dianion of trithiocarbonic acid.[27,29] IIIa was suggested to occur as an intermediate in insertion reactions of CS_2 into metal–thiolate bonds and to rearrange rapidly in order to form the more stable type IIb.[27]

Accordingly, in $[\{Ru(PPh_3)\}(\mu\text{-}'S_4'CS_2)\{Ru(PPh_3)'S_4'\}]$ (**3**) the new type of thioxanthate complex IIIb could be stabilized and characterized for the first time.

Addition of CS_2 to a $[Ru(PPh_3)'S_4']$ fragment by nucleophilic attack of one of both thiolate atoms to the carbon atom of CS_2 may yield the intermediate $[Ru(PPh_3)'S_4'CS_2]$ with a type IIIa ligand according to eq 9.

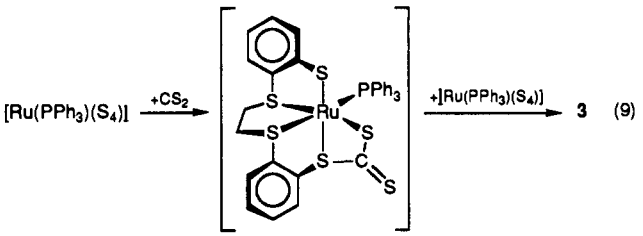

Because the respective thiolate atom is part of the tetradentate 'S_4' ligand, rearrangement of the labile type IIIa into type IIb is prevented and coordination of another $[Ru(PPh_3)'S_4']$ fragment to the thiocarbonyl S atom finally leads to **3**. The primary addition of CS_2 to $[Ru(PPh_3)'S_4']$ fragments is rendered possible by the high nucleophilicity of the 'S_4' thiolate donors.[30]

As discussed above, the formation of **3** from racemic $[Ru(PPh_3)'S_4']$ fragments according to Scheme I is expected to yield two diastereomeric pairs of enantiomers. They indeed form as can be deduced from the four signals in the $^{31}P\{^1H\}$ NMR spectra of the deep red solutions of $[Ru(PPh_3)'S_4']_x$ in CS_2 (Figure 1), and the *RS*/*SR* pair of enantiomers of **3** could be characterized by X-ray structure determination.

The assumption that CS_2 reversibly adds to $[Ru(PPh_3)'S_4']$ fragments is corroborated by the rapid formation of **2**·CS_2 according to eq 7 as well as the fact that **3** dissolves only in CS_2 without decomposition. Other solvents cause rapid decomposition of **3**.

Summary

$[Ru(SH_2)(PPh_3)'S_4']$·THF (**1**·THF) is the first H_2S complex that could be characterized by X-ray crystallography. **1**·THF shows that H_2S in complexes with sulfur-dominated coordination spheres is stabilized by strong hydrogen bonds. Their strength results on one hand from the high charge density in the [RuS] framework, through which the thiolate donors become good hydrogen acceptors, and on the other hand from the large polarity of the S–H bond in coordinated H_2S. Short S···S distances and the low ν(S–H···S) frequency prove that S–H···S bridges can be significantly more stable than hitherto assumed. This result is of considerable interest because S–H···X bridges (X = N, O, S) in ferredoxines and many other metal–sulfur enzymes influence redox potentials, equilibrium configurations, and consequently reactivities.[31]

Oxidation of yellow **1** yields deep turquoise-blue $[(\mu\text{-}S_2)\{Ru(PPh_3)'S_4'\}_2]$ (**2**). **2** also forms from $[Ru(PPh_3)'S_4']$ fragments and other sources of sulfur such as S_8, NBu_4SH, or CS_2 and can exist in two diastereomeric forms which both were characterized by X-ray crystallography. The RuSSRu core in **2** is a chromophore and can be described as a 4c–6e π system. It causes intense absorptions which reach into the near-IR region of the electronic spectrum.

Addition of CS_2 to S(thiolate) donors of $[Ru(PPh_3)_2'S_4']$ fragments leads to formation of deep red $[\{Ru(PPh_3)\}(\mu\text{-}'S_4'\text{-}CS_2)\{Ru(PPh_3)'S_4'\}]$ (**3**) which contains a bridging thioxanthate ligand in an unprecedented bonding mode.

1 and **2** as well as **3** show how small sulfur-containing molecules can be coordinated to and stabilized by metal centers in sulfur-

(27) Shaver, A.; Plouffe, P.-Y.; Bird, P.; Livingstone, E. *Inorg. Chem.* **1990**, *29*, 1826 and literature reported therein.
(28) Coucouvanis, D. *Progr. Inorg. Chem.* **1979**, *26*, and literature reported therein.
(29) Fehlhammer, W. P.; Mayr, A.; Stolzenberg, H. *Angew. Chem.* **1979**, *91*, 661; *Angew. Chem., Int. Ed. Engl.* **1979**, *18*, 626.
(30) Sellmann, D.; Lechner, P.; Moll, M.; Knoch, F. *Z. Naturforsch.*, in press.
(31) Nakamura, A.; Ueyama, N. In *Metal Clusters in Proteins*; Que, L., Ed.; American Chemical Society: Washington, DC, 1988; Chapter 14.

dominated coordination spheres. These results may contribute to answer the question why nature uses in enzymes like nitrogenases or hydrogenases transition metals and sulfur ligands for the active centers in order to generate catalysts that render possible the most difficult reactions even under the mildest conditions.

Acknowledgment. We thank W. Preetz, Institut für Anorganische Chemie, Universität Kiel, for Raman measurements. These investigations were supported by the Deutsche Forschungsgemeinschaft, by the Fonds der Chemischen Industrie, and by a donation of $RuCl_3 \cdot xH_2O$ by Degussa AG, Hanau. We gratefully acknowledge this support.

Registry No. 1·THF, 132699-25-3; **2**, 127139-84-8; $2 \cdot CH_2Cl_2$, 138052-72-9; $2 \cdot CS_2$, 138052-73-0; **3**, 138052-71-8; $3 \cdot CS_2$, 138128-09-3; $[Ru(PPh_3)'S_4']_x$, 124401-90-7; $H_2'S_4'$, 83209-89-6; CS_2, 75-15-0.

Supplementary Material Available: Listings of isotropic thermal parameters, anisotropic displacement parameters, bond distances as well as bond angles of 1·THF, $2 \cdot CS_2$, and $3 \cdot CS_2$, and coordinates of hydrogen atoms of 1·THF and $2 \cdot CS_2$ (35 pages); listings of F_o and F_c values (24 pages). Ordering information is given on any current masthead page. Further details of the X-ray crystal structure analyses have been deposited and can be obtained from the Fachinformationszentrum Energie, Physik, Mathematik, D-7514 Eggenstein-Leopoldshafen 2 by citing the deposition numbers CSD 320193 ($[Ru(SH_2)(PPh_3)'S_4']\cdot THF$ (1·THF)), CSD 320250 ($[(\mu\text{-}S_2)\{Ru(PPh_3)'S_4'\}_2]\cdot CS_2$ ($2 \cdot CS_2$)), CSD 320249 ($[\{Ru(PPh_3)\}(\mu\text{-}'S_4'CS_2)\{Ru(PPh_3)'S_4'\}]\cdot CS_2$ ($3 \cdot CS_2$)), the authors, and the reference.

Conformation of Pt(dien)[d(ApGpA)-*N*7(2)] in the Solid State and in Aqueous Solution, As Determined with Single-Crystal X-ray Diffraction and High-Resolution NMR Spectroscopy in Solution

Gert Admiraal, Maarten Alink, Cornelis Altona, Fransje J. Dijt, Carla J. van Garderen, Rudolf A. G. de Graaff, and Jan Reedijk*

Contribution from the Department of Chemistry, Gorlaeus Laboratories, Leiden University, P.O. Box 9502, 2300 RA Leiden, The Netherlands. *Received June 26, 1991*

Abstract: The structure in the solid state and in solution of the adduct between $Pt(dien)^{2+}$ and the trinucleotide d(ApGpA), Pt(dien)[d(ApGpA)-*N*7(2)], has been studied with high-resolution NMR techniques and X-ray diffraction. This adduct is a model for the intermediate in the binding of the antitumor drug *cis*-$PtCl_2(NH_3)_2$, cisplatin, to DNA. In aqueous solution the intramolecular interactions between the guanine residue and the 3′ adenine are reduced upon platination, while the stacking between the 5′ adenine and guanine remains intact. Furthermore, binding of the monofunctional platinum compound to the N7 of guanine results in a change in the sugar conformation of all three residues. Instead of the usual 80–100% *S* conformation, all three Pt(dien)[d(ApGpA)-*N*7(2)] deoxyribose rings are in an almost 50% N/S equilibrium. The change of the sugar conformation causes a change in the DNA backbone; this change seems to be the reason for the more easy Pt binding at the 5′ side of the molecule. The conformational changes were found to be sequence dependent as seen from comparison with Pt(dien)[d(CpGpT)-*N*7(2)]. In that case the conformation of only the guanine residue is changed upon platinum binding. Crystallographic data of Pt(dien)[d(ApGpA)-*N*7(2)] are as follows: space group $P2_12_12_1$, $Z = 8$, $a = 20.094$ (5) Å, $b = 21.418$ (5) Å, $c = 29.631$ (6) Å, $V = 12752$ Å^3, resolution = 1.15 Å, $R_w = 0.087$ for 4855 reflections and 776 variables. Apart from two Pt(dien)[d(ApGpA)-*N*7(2)] molecules 18 well-ordered water molecules are present in the asymmetric unit. The two independent molecules which have a similar conformation are held together in the unit cell by stacking interactions and hydrogen bonding of the bases. Characteristic features are unusual G·G base pairs (using N3 and N2, N···N = 2.84–2.99 Å) and A·A base pairs (using N6 and N1 of A(1), i.e. the 5′ adenine, N···N distances are 2.80 and 3.04 Å; and also using N6 and N7 of A(3), N···N = 2.96–2.99 Å). These G·G and A·A base pairs are stacked in the *b* direction of the crystal. The backbone of each d(ApGpA) molecule has an extended conformation. The only intramolecular interactions are relatively weak H bridges between an amine ligand and a phosphate oxygen and between another amine ligand and a guanine O6 (N···O = 3.10–3.15 Å). Such an intramolecular interaction has been observed earlier in the crystal structure of *cis*-$Pt(NH_3)_2$[d(CpGpG-N7(2),N7(3)]. The intermolecular interactions (i.e. the crystal packing effects) are clearly stronger than the stacking forces within a molecule, resulting in different molecular structures and conformations in solution and in the crystal.

Introduction

It is well-known that the antitumor drug cisplatin (*cis*-$PtCl_2(NH_3)_2$, cDDP[1]) forms a didentate complex with DNA.[2-4] Studies on the enzymatic digestion of platinated salmon sperm DNA[2] show a perference of cDDP for two neighboring guanines (about 65% of the DNA-bound platinum), while binding occurs at the N7 position of the bases (a -GpG-N7,N7 chelate). A smaller amount (up to 20%) of an -ApG-N7,N7 chelate is formed. In contrast, the -GpA-N7,N7 chelate has not yet been found in DNA. Also two minor platinum-containing compounds were found, i.e. monofunctionally bound $Pt(NH_3)_3$dGMP (2%) and *cis*-$Pt(NH_3)_2(dGMP)_2$ (13%). This last adduct originates from both interstrand cross-links and enzymatically degraded d(Gp{Np}$_n$G), $n \geq 1$, in which platinum is bound to two guanines with one or more nonbound bases in between. The monofunctional adduct at a guanine-N7 is thought to be an intermediate in the

(1) Abbreviations: cisplatin, cDDP, *cis*-$PtCl_2(NH_3)_2$; d(ApGpA), deoxyadenylyl(3′-5′)deoxyguanylyl(3′-5′)deoxyadenosine; dien, diethylenetriamine; NMR, nuclear magnetic resonance; pH*, uncorrected meter reading of solutions of D_2O; TMA, tetramethylammonium chloride; TMP, trimethylphosphate.

(2) Fichtinger-Schepman, A. M. J.; van der Veer, J. L.; den Hartog, J. H. J.; Lohman, P. H. M.; Reedijk, J. *Biochemistry* **1985**, *24*, 707-713.

(3) Inagaki, K.; Kidani, Y. *Inorg. Chim. Acta* **1985**, *106*, 187-191.

(4) Pinto, A. L.; Lippard, S. J. *Biochim. Biophys. Acta* **1985**, *780*, 167-180.

0002-7863/92/1514-930$03.00/0